Radiotherapy and Oncology 132 (2019) 257–265

Contents lists available at ScienceDirect

Radiotherapy and Oncology

journal homepage: www.thegreenjournal.com

Original Article

Quantification of cardiac subvolume dosimetry using a 17 segment model of the left ventricle in breast cancer patients receiving tangential beam radiotherapy

Simon Tang [a,b,c,*], James Otton [b,d], Lois Holloway [a,b,c,e], Geoffrey P. Delaney [a,b,c], Gary Liney [a,b,c], Armia George [c], Michael Jameson [a,b,c], David Tran [e], Vikneswary Batumalai [a,c], Liza Thomas [b,e,f], Eng-Siew Koh [a,b,c]

[a] Ingham Institute of Applied Medical Research, Liverpool Hospital; [b] University of New South Wales; [c] Cancer Therapy Centre, Liverpool Hospital; [d] Department of Cardiology, Liverpool Hospital, Australia; [e] University of Sydney; and [f] Department of Cardiology, Westmead Hospital, Australia

ARTICLE INFO

Article history:
Received 19 December 2017
Received in revised form 23 September 2018
Accepted 27 September 2018
Available online 13 November 2018

Keywords:
Breast cancer
Cardiotoxicity
Deep inspiration breath hold
Radiotherapy

ABSTRACT

Purpose: Subacute changes following breast radiotherapy have been demonstrated in discrete areas of the left ventricle (LV), with recent guidelines being developed to help determine dose to subvolumes of the LV. This study aims to determine doses to the 17 segments of the LV as per the American Heart Association (AHA) and other cardiac subvolumes, and to correlate mean heart (MHD) dose with various subvolume dosimetric indices. These results may direct focus to specific left ventricular segments in studies of radiation-related heart disease incorporating surveillance imaging, help to determine more precise dose response relationships, and potentially aid prediction of late radiation effects.

Methods and materials: The heart and cardiac subvolumes of 29 patients treated with tangential radiotherapy for left breast cancer were contoured. Delineation of cardiac subvolumes (cardiac chambers, cardiac valves and the 17 segments of the LV) was undertaken using a novel contouring method on planning CT data reformatted into the cardiac axis. Individual segments were then combined to determine doses to the basal, mid and apical left ventricular regions, and the anterior, septal, inferior and lateral ventricular walls. Radiotherapy doses (including maximum, mean, D1cc, V25) were determined. Correlation analyses were performed between MHD and various substructure dosimetric indices.

Results: Twenty five patients received tangential breast free breathing radiotherapy alone, and four patients received regional nodal irradiation including the internal mammary chain with deep inspiration breath hold (DIBH). For patients receiving breast only radiation, the median mean heart radiation dose was 2.62 Gy (range 1.52–3.90 Gy), and a heterogeneous dose distribution to the LV was noted, with the apical region receiving the highest median mean dose (14.99 Gy) compared with the mid and basal regions (3.10 Gy and 1.51 Gy respectively). The anterior LV wall received the highest median mean dose (9.21 Gy) with the remaining walls receiving similar mean doses (range 1.79–3.05 Gy). The anterior LV apical segment (segment 13) and apex (segment 17) received the highest individual median mean segment doses (26.73 Gy and 30.02 Gy respectively). Apical segments received the highest median mean doses (segments 13, 14, 15, 16), followed by the mid anterior (segment 7) and anteroseptal (segment 8) segments. Segments receiving the highest doses remained unchanged between the DIBH cohort and free breathing cohort. MHD showed a high correlation with the anterior wall $r = 0.71$, $p < 0.05$ and entire left ventricle $r = 0.82$, $p < 0.05$, but correlations varied from weak to high when MHD was correlated with segments receiving highest doses (range $r = 0.43$–0.76), $p < 0.05$.

* Corresponding author at: Ingham Institute for Applied Medical Research, 1 Campbell Street, Liverpool, Australia.
E-mail address: Simon.Tang@health.nsw.gov.au (S. Tang).

https://doi.org/10.1016/j.radonc.2018.09.021

Conclusions: In the setting of breast cancer radiotherapy, there are substantial RT dose variations within specific LV segments, with mid and apical anterior ventricular segments (segments 7, 13) and the apical region of the LV (segments 13, 14, 15, 16, 17) being consistently exposed to the highest radiation doses. Determining segmental and regional RT doses to the left ventricle may help guide focus in diagnostic cardiology in the post radiotherapy setting.

Radiotherapy and Oncology 132 (2019) 257–265

An increased incidence of cardiovascular disease (CVD) following radiotherapy [1,2], particularly in patients with left sided breast cancer [3] has been reported. Darby et al. [4] demonstrated a 7.4% increase in rate of major coronary events occurred with every Gray increase in mean heart dose (MHD).

The heart is comprised of myocardium, connective, pericardial, and vascular tissues, which are composed into chambers, arteries and valves. The spectrum of late cardiovascular diseases including congestive cardiac failure, valvular dysfunction, coronary artery disease [5] and very rarely constrictive pericardial disease [6], combined with animal studies suggesting differing radiosensitivity of constituent cardiac tissues [7], suggests that a variety of dose constraints might be required [8].

MHD has been the preferred radiotherapy dose-volume metric against which cardiac outcomes have been measured. It is ubiquitously reported allowing straightforward cross study comparisons [9], has low inter-observer variability [10], and is a proven measure in the development of dose-response relationships [4,11], despite heterogeneous dose distributions to the heart [12], and differing radiosensitivities of cardiac tissues [7]. Moreover the estimated MHD remains constant throughout the cardiac cycle, unlike that of the distal left anterior descending artery [13] hence making MHD a more robust metric. Also, smaller cardiac subvolumes are associated with greater inter-observer variability with low concordance index and percent contour overlap values [14]. However, MHD may not be the most sensitive metric to describe exposure and predict for late RT effects. Hahn et al. [15] have demonstrated superiority of coronary artery dose variables to mean heart dose when modelling variables to late ischemic cardiac events. Van den Bogaard et al. [16] have suggested the left ventricular V5 is a more sensitive predictor than MHD for acute coronary events. Such examples highlight the limitations of using MHD as the preferred predictive index for future cardiovascular disease.

Cardiac imaging studies too have increasingly documented discrete focal changes within the heart. A reduction in left ventricular myocardial strain using advanced echocardiographic techniques was detected following breast radiotherapy in left sided cancer patients [11,17], with the greatest decrement seen in the apical segments [18]. Perfusion studies [19,20] have displayed focal left ventricular abnormalities following tangential breast radiotherapy. Correa et al. [21] have documented discrete areas of coronary artery stenosis present in left breast cancer patients.

It has been long recognised that an improved understanding of radiation dose effect would require a more detailed assessment of radiation dose to cardiac subvolumes [8]. To address this, a number of cardiac atlases [14,22] have been published recommending the delineation of cardiac subvolumes, including specific regions of the left ventricular wall. Using these methods, one study has demonstrated an association between left ventricular segmental radiation dose and corresponding late cardiac left ventricular segmental injury [2], consistent with previously reported findings correlating left ventricular segmental radiation dose with reduction segmental ventricular strain [18]. In addition, in a retrospective spatial dosimetric analysis of 1101 lung cancer patients, McWilliam et al. [23] identified a region at the base of the heart, which when higher doses were delivered to, were associated with higher patient mortality. These studies in combination, are suggestive of a dose response relationship occurring at the cardiac subvolume level, and do not exclude the possibility of more critical or radiosensitive cardiac subvolumes. Therefore an improved understanding of the dose-cardiotoxicity relationship is required in guiding radiation therapy delivery especially in the era of intensity modulated radiotherapy and image guidance, where dose sensitive structures can be visualised and deliberately avoided.

The purpose of this study was to primarily demonstrate the utility of a novel contouring technique which could be used to determine radiation dose to discrete regions of the left ventricle as defined by the American Heart Association (AHA) 17 segment model [24]. This same technique was also used to delineate the cardiac valves and chambers with more accuracy. Secondly correlative analyses were performed, examining the relationship between various dosimetric parameters within a single structure (e.g. whole heart, coronary artery, or left ventricular segment), as well has relating MHD to other structures' dosimetric parameters (e.g. left ventricular V5, left ventricular D50 etc.).

Materials and methods

Patient selection

Breast cancer patients undergoing tangential left breast radiotherapy were prospectively recruited during the period from October 2015 to October 2016.

Computed tomography (CT) imaging acquisition process

All patients were simulated in a semi-recumbent supine position, immobilised in a breast jig and vacuum bag. Routine planning CTs undertaken on a Phillips Brilliance Big Bore 16 slice CT scanner (Amsterdam, Netherlands) were used for cardiac delineation (non contrast and non ECG gated) acquired at 2 mm slice thickness. The imaging datasets were transferred to the Oncentra Brachytherapy software v4.5.2 (Elekta, Stockholm, Sweden), and reformatted into the cardiac planes to generate the cardiac short axis, 2 chamber and 4 chamber apical views (see Fig. 1). Rotation was applied to only one plane at a time. The cardiac chambers, valves, and 17 segments of the left ventricle as per the AHA model [14] were then contoured in these planes.

The whole heart and coronary arteries were contoured in the standard orthogonal (axial) plane. The basal, mid and apical left ventricular regions were formed by summing segments 1–7, 8–12, and 13–17 respectively [24]. The anterior wall was generated by combining the anterior segments (1, 7, 13), septal wall by combining the anteroseptal (2, 8), inferoseptal (3, 9) and apical septal (14) segments, the inferior wall by combining the inferior segments (4, 10, 15), and the lateral wall by combining the anterolateral (6, 12), inferolateral (5, 11) and apical lateral (16) segments.

This RT structure dataset was then imported into Pinnacle v9.10 where dose was calculated (see Fig. 2). MIM software v6.77 (Mim

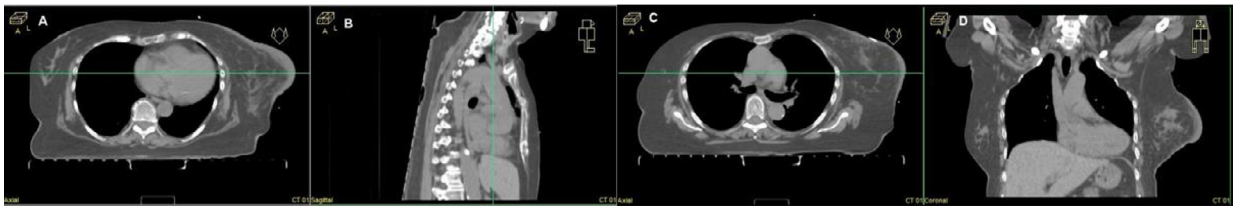

The above panels represent a patient in standard orthogonal views. Panels A, B, and D are axial, sagittal, and coronal slices of the patient respectively. Panel C will serve as a reference axial slice.

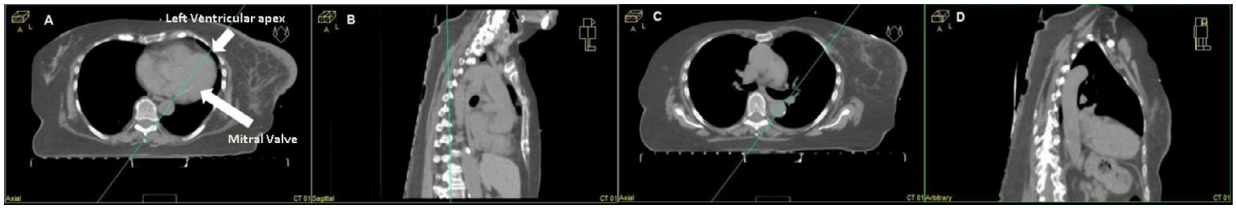

The index slice is at the level of the mitral valve seen in axial plane (Panel A). The coronal plane (Panel D) is then rotated into a plane that passes through the centre of the mitral valve and left ventricular apex seen in Panel A. Note during the entire process, only one plane is rotated at a time.

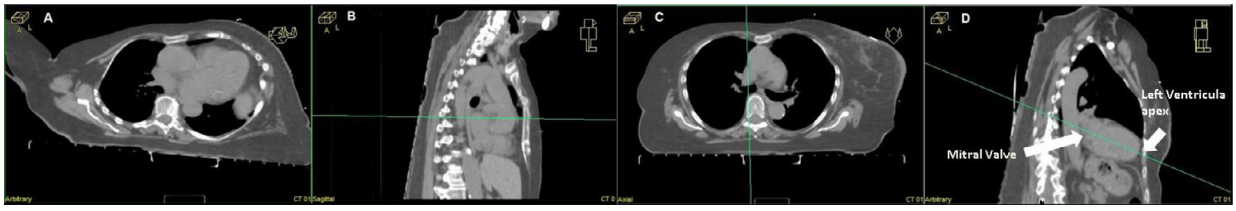

Panel A is then rotated into a plane that passes through the mitral valve and left ventricular apex in the plane shown in Panel D

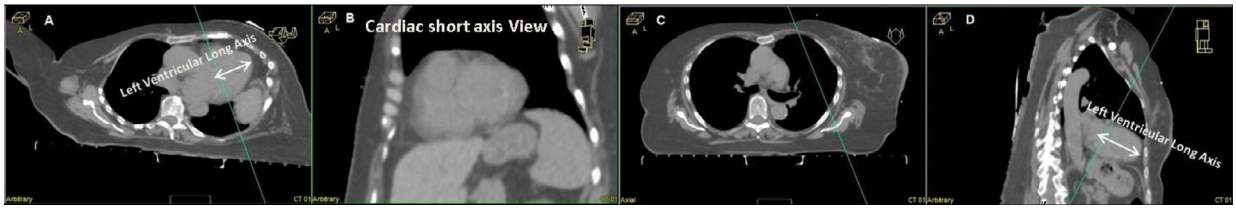

The sagittal plane (Panel B) is then rotated into a plane that is perpendicular to the left ventricle along its long axis as seen in Panel A and Panel D. This generates the cardiac short axis seen in Panel B.

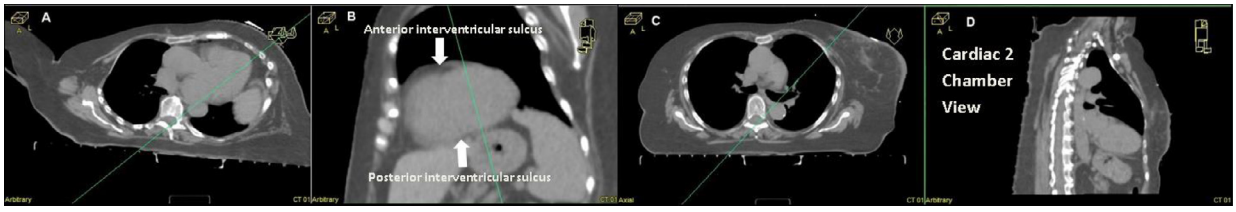

Panel D is then rotated into a plane that is parallel to a line between the anterior and posterior interventricular sulcus in Panel B at the level of the mid ventricle. This generates the 2 chamber view in Panel D.

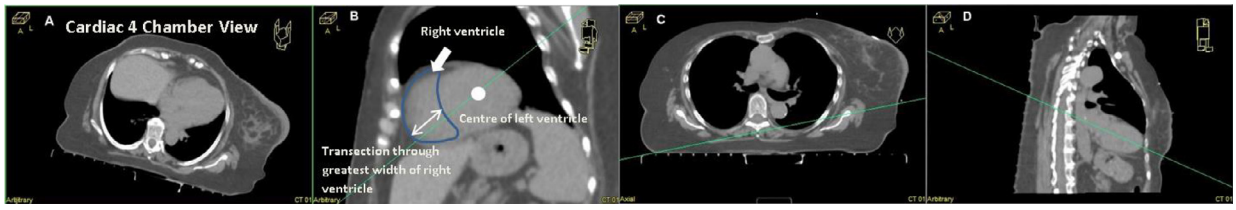

Panel A is then rotated in a plane at the mid level of the left ventricle in Panel B. A line from an imaginary point at the centre of the left ventricle is then extended transecting the right ventricle at its greatest width. The right ventricle is highlighted in blue for clarity.

Fig. 1. Cardiac axis generation.

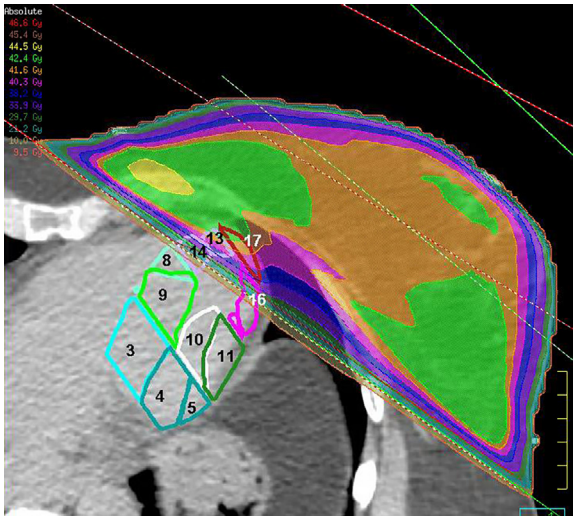

Fig. 2. Interpolated segmental contours transferred into Pinnacle Treatment Planning software. Left ventricular segments are numbered above. Tangential breast radiation can be seen to predominantly affect the apical segments 13, 14, 15, 16 and 17.

Software Inc, Cleveland, Ohio) was used to read out dosimetric data.

Cardiac structure delineation

The whole heart was contoured as per the RTOG consensus guidelines [14]. The cardiac chambers were contoured in the short axis[1] view. Anterior interventricular grooves allowed demarcation between left and right ventricles. Atrioventricular grooves provided demarcation between atria and ventricles. Mitral and tricuspid valves were delineated as a 1 cm structure saddling their respective atria and ventricle. The aortic valve was generally well visualised, with the proximal 1 cm of the pulmonary trunk contoured as an approximation of the pulmonary valve. The cardiac 2 chamber[2] and 4 chamber[3] views were used to verify atrial and ventricular contours (see Fig. 3).

When contouring the ventricular segments, the left ventricle was divided into basal, mid and apical regions. The apical region was defined as the summation of the apical cap (segment 17) and segments 13–16. The apical cap was defined first as the apical 1 cm of the ventricle. The remaining left ventricle was then divided into thirds, consisting of the basal, mid and remaining apical regions. The basal and mid regions were carefully divided into six segments, and the remaining apical region divided into four segments, to best approximate those outlined in the AHA 17 segment model [24]. The interventricular septum provided an anchoring point to ensure correct orientation of the segments when contouring. Normal female ventricular wall thickness ranges between 6–9 mm [25], and therefore a contoured ventricular wall thickness of 9 mm for the basal and mid regions, and 6 mm for the apical region was used, acknowledging the tapering myocardial thickness along the ventricular axis. Contours were performed by a single observer. The first 10 cases were audited and verified by the study cardiologist (JO).

The position of the coronary vessels was inferred using anatomical landmarks as described by Duane et al. [22]. The right and left atrioventricular grooves were used as a surrogate for the left circumflex and right coronary arteries respectively, and the interventricular groove for the left anterior descending artery. The left coronary artery was identified and contoured until it diverged into the left atrioventricular and interventricular grooves. Angiographic data have demonstrated that the average female proximal coronary artery radial diameter is 3.2 mm [26], and given the tapering nature of coronary vessels, a contouring circle of 3 mm was used to delineate coronary vessels.

Radiotherapy technique

Patients undergoing breast only radiotherapy were treated with free breathing medial and lateral tangents that adequately covered the breast planning target volume (PTV). Medial and posterior tangential field edges were generally the midline and mid axillary line respectively, however field edges were modified based on PTV coverage and disease risk. The posterior field borders were aligned. A departmental mean heart dose constraint of <4 Gy was used to plan all cases with no deliberate cardiac shielding. All patients receiving breast/chest wall only radiation were treated free breathing. A detailed description of the radiation therapy technique for patients receiving nodal irradiation is provided in the Supplementary Material.

All patients were planned to 42.4 Gy in 16 fractions or 50 Gy in 25 fractions according to radiation oncologist preference. Electron boost irradiation doses were not included in the final dosimetric analysis as it contributes minimally, if at all, to the overall heart dose (18), with the exception of one patient who received a simultaneous integrated photon boost.

Absolute doses were reported, as well as EQD2 (equivalent dose in 2 Gy per fraction) conversions using the Linear Quadratic (LQ) formulae. EQD2 conversion was performed in MiM 6.7.7 (MiM Software, Cleveland, USA), with an α/β of 3 for late reacting tissues. Given the exploratory nature of the analysis, reported values not only include mean and maximum doses, but also V3 [27], V5 to V50 in 5 Gy increments (including V25 and V30 [8]), D50, D90, D95, D98 and D2cc values. Select correlations between the different dose metrics were performed using the computing environment R (R Development Core Team, 2005) and provided as Supplementary Material. Additional software packages (Corrplot) were used.

All doses have been reported as median doses. The abbreviated results published are in absolute dose. A more complete list and EQD2 dose conversations have been provided as Supplementary Material.

Statistical considerations

Pearson's correlation between dose metrics was performed in patients receiving free breathing tangential breast radiotherapy alone. Correlations between dosimetric parameters for each subvolume, MHD and mean values for all subvolumes, and MHD and all dosimetric parameters for selected subvolumes were performed. A p value ≤ 0.05 was considered statistically significant. Definitions of low, moderate, high and very high correlations are defined as 0.3–0.5, 0.5–0.7, 0.7–0.9, and 0.9 to 1 respectively [28].

Results

Patient Population

A total of 29 patients were recruited. Twenty five patients received tangential radiotherapy to the breast alone whilst free breathing, three patients received tangential breast and regional nodal irradiation using DIBH, and one patient received post

[1] The cardiac short axis view displays the cross section of the left and right ventricle

[2] The cardiac 2 chamber view displays the left atrium and left ventricle.

[3] The cardiac 4 chamber view projects the right atrium, right ventricle, left atrium and left ventricle simultaneously

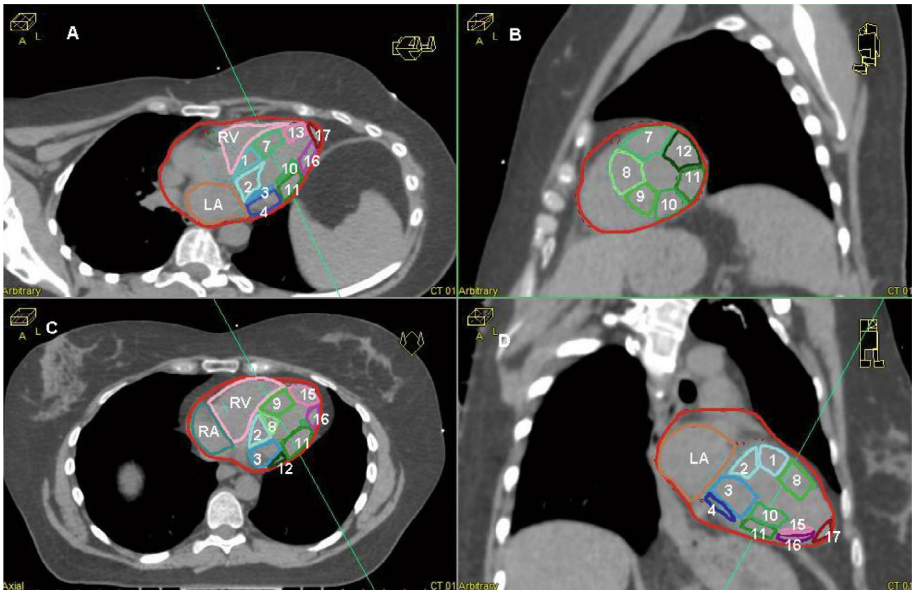

Fig. 3. Left Ventricular Segments in 4 Chamber (A), Short Axis (B), standard axial plane (C), and 2 Chamber (D) views. This patient was contoured in Oncentra Brachytherapy before being imported into Pinnacle Treatment Planning Software. Panels A, B, D display the cardiac 4 chamber, short axis, and 2 chamber views. Panel C displays the standard axial slice for reference. Left ventricular segments were contoured in the cardiac short axis (Panel B), before being interpolated into standard axial planes. Panel B demonstrates the cross section of the left ventricle at the mid-level. The circumferential extent of the left ventricle is visualised more clearly in the short axis (Panel B), with the superior and apical aspect of the left ventricle being best visualised in the cardiac 4 chamber (Panel A) and 2 chamber views (Panel D). LA = left atrium, RA = right atrium, RV = right ventricle. The numbers above represent the various left ventricular segments. 1, 2, 3, 4, 5 and 6 represent the basal anterior, basal anteroseptal, basal inferoseptal, basal inferior, basal posterolateral, and basal anterolateral left ventricular wall. 7, 8, 9, 10, 11, and 12 represent the mid anterior, mid anteroseptal, mid inferoseptal, mid inferior, mid inferolateral, and mid anterolateral left ventricular wall. Segments 13, 14, 15 and 16 represent the apical anterior, apical septal, apical inferior and apical lateral left ventricular wall. Segment 17 represents the apical cap.

mastectomy radiotherapy as well as regional nodal irradiation using DIBH. Regional nodal irradiation included the supraclavicular fossa and internal mammary chain.

Dose to the whole heart

The median MHD was 2.62 Gy (range 1.52–3.90 Gy) in patients who received free breathing tangential breast radiotherapy only. The median MHD was 2.60 Gy (range 2.00–2.87 Gy) for patients who received additional nodal irradiation using a DIBH technique.

Dose to the left ventricular walls, regions, and segments

Table 1 provides a detailed summary of dose to the cardiac segments and walls. For patients treated with free breathing tangential radiation, median maximum doses to the left ventricular walls were greatest in the anterior, septal and lateral walls (range 39.20–41.68 Gy) when compared with the median maximum dose delivered to the inferior wall (16.13 Gy). Median mean dose however was highest in the anterior wall (9.21 Gy) compared to the lateral and septal walls (3.05 Gy and 2.96 Gy respectively). The inferior wall received a median mean dose of 1.79 Gy. Volumetric indices indicate that the anterior wall consistently receives higher doses at greater volumes (see Supplementary Index).

The three regions of the heart, (basal, mid and apical regions) highlighted the spatial differences in ventricular radiotherapy exposure. For patients receiving breast radiation only, the basal region received a median mean and median maximum dose of 1.51 Gy and 4.05 Gy, the mid region 3.10 Gy and 31.41 Gy, and the apical region 14.99 Gy and 42.10 Gy respectively. The segments of the left ventricle mirrored the above findings, with the anterior and apical segments receiving the highest doses (segments 7, 13, 14, 15, 16 and 17) (see Fig. 2).

Dose to cardiac chambers, valves and coronary arteries

Doses to the cardiac chambers and valves for both the breast only and regional nodal radiotherapy groups are reported in the Supplementary Material. Dose delivered to the left anterior descending artery was highest with a median mean and median maximum dose of 18.11 Gy and 41.09 Gy respectively for breast irradiation alone patient, and 7.47 Gy and 21.39 Gy respectively for those receiving nodal irradiation. The remaining arteries received substantially less radiation doses. Further details of dose delivered to the coronary arteries are summarised in Table 1.

Comparison of doses delivered in breast only and DIBH techniques.

The median MHD (2.62 Gy vs 2.60 Gy) was comparable between the free breathing tangential breast radiotherapy group ($n = 25$) and DIBH cohort ($n = 4$), despite the use of modified wide tangents to cover the IMC. Segments receiving the highest doses remained unchanged between the DIBH cohort and free breathing cohort, with apex (17), apical region (13, 14, 15, 16), anterior (7) and anteroseptal (8) mid segments receiving the highest doses.

Correlation of dose metrics within MHD and other contours

MHD correlated (moderate to very highly) with dosimetric (D1cc, D2cc, D50, D90, D95, D98), and volumetric measurements (V5, V10, V15, V20, V25, V30, V35 and V40) (see Fig. 4). Maximum dose correlated strongly only with V3 and V5. Minimum dose correlated generally highly to very highly with D90, D95, D98. Correlations within similar dosimetric descriptors (i.e. V5, V10, V15, V20, and V30 correlated very highly with one another). This trend was also seen in broadly for all cardiac substructures; for example the apical mean dose correlated strongly with V10–V40, and D1cc–D98, with maximum doses correlating strongly with

Table 1
Selected Radiation Dose metrics delivered to the AHA 17 Segments, Regions, and Walls of the Left Ventricle.*

Structure	Mean (Gy)		Maximum (Gy)	
	Breast Only (Free Breathing)	Breast + Nodes (DIBH)	Breast Only (Free Breathing)	Breast + Nodes (DIBH)
Coronary Arteries				
Right Coronary	0.96 (0.40–1.97)	1.34 (1.00–1.85)	1.36 (0.50–2.40)	2.32 (1.99–3.18)
Left Anterior Descending	**18.11 (4.12–30.51)**	**7.47 (4.07–20.01)**	**41.09 (18–44.12)**	**21.39 (8.80–47.65)**
Left Circumflex	0.98 (0.43–1.23)	1.17 (1.01–2.63)	1.56 (0.68–2.20)	2.19 (1.81–7.78)
Left Coronary Artery	1.04 (0.50–1.94)	1.91 (1.11–2.35)	1.34 (0.63–2.35)	2.41 (1.82–2.61)
Basal Segments				
1	**2.15 (1.17–3.74)**	**2.61 (2.17–3.01)**	**4.06 (1.96–18.81)**	**4.51 (3.32–7.78)**
2	1.87 (1.06–2.66)	2.18 (1.98–2.23)	3.23 (1.83–15.08)	3.67 (3.03–4.75)
3	1.21 (0.74–1.62)	1.31 (1.18–1.56)	1.97 (1.25–2.72)	2.08 (1.80–2.35)
4	0.97 (0.51–1.44)	0.97 (0.86–1.39)	1.5 (0.88–2.51)	1.57 (1.26–1.95)
5	1.12 (0.57–1.87)	1.13 (0.92–1.50)	1.65 (0.91–3.27)	1.80 (1.51–1.96)
6	1.60 (0.97–2.38)	1.98 (1.46–2.11)	2.88 (1.71–6.97)	4.04 (2.80–4.69)
Mid Segments				
7	**5.10 (2.96–19.24)**	**4.40 (2.82–5.83)**	**31.24 (5.84–40.37)**	**14.10 (4.26–30.03)**
8	3.45 (2.19–7.8)	3.26 (2.56–3.77)	15.98 (3.66–39.59)	6.07 (3.81–9.37)
9	2.19 (1.38–3.03)	2.16 (1.56–2.31)	3.32 (2.20–6.24)	3.23 (2.13–3.34)
10	1.71 (0.98–2.68)	1.57 (1.16–1.80)	2.73 (1.90–4.65)	2.70 (1.76–2.87)
11	1.94 (1.17–3.08)	1.96 (1.34–2.3)	3.34 (2.13–17.47)	3.03 (2.02–4.35)
12	2.98 (1.75–7.01)	3.00 (2.04–3.87)	8.78 (3.05–36.75)	7.38 (3.5–11.59)
Apical Segments				
13	**26.73 (12.23–38.04)**	**11.95 (3.83–21.68)**	**41.59 (35.82–48.00)**	**26.02 (6.52–45.65)**
14	8.23 (2.49–20.88)	3.64 (2.48–4.87)	39.83 (4.01–42.58)	10.55 (3.86–26.99)
15	3.61 (2.09–9.54)	2.48 (1.82–3.08)	15.85 (3.17–38.72)	3.89 (2.63–7.02)
16	11.19 (3.91–23.99)	5.22 (2.62–7.85)	39.14 (22.44–46.51)	17.72 (4.82–37.45)
Apex				
17	**30.02 (3.68–41.83)**	**8.83 (3.07–23.23)**	**42.04 (20.2–47.44)**	**21.55 (5.81–47.62)**
Ventricular Walls				
Anterior	**9.21 (4.63–18.25)**	**5.45 (3.00–7.97)**	**41.68 (35.59–48.00)**	**26.08 (6.81–46.31)**
Septal	2.96 (1.55–6.03)	2.48 (1.96–2.81)	39.83 (4.05–42.58)	11.05 (3.86–27.94)
Inferior	1.79 (1.08–3.76)	1.61 (1.31–1.74)	16.13 (3.17–38.90)	3.83 (2.63–7.44)
Lateral	3.05 (1.80–7.18)	2.59 (1.71–3.19)	39.20 (23.85–46.58)	17.58 (4.82–38.65)
Ventricular Regions				
Basal	1.51 (0.90–2.07)	1.80 (1.46–1.91)	4.05 (1.92–20.65)	4.49 (3.30–8.10)
Mid	3.10 (2.17–6.66)	2.77 (1.98–3.39)	31.41 (6.01–40.61)	14.82 (4.26–30.07)
Apical	**14.99 (3.81–24.21)**	**6.31 (2.88–11.32)**	**42.10 (35.59–48.00)**	**26.08 (6.81–47.62)**

Segments, walls or regions with the highest doses have been bolded.
* All doses reported are median values.

V3 and V5, and minimum doses correlating strongly with D90–D98. Additional correlation plots have been provided in the Supplementary Index.

This pattern of correlation between mean, maximum and minimum doses to various dosimetric and volumetric indices also applied broadly individual ventricular segments.

Correlation of mean heart dose with specific cardiac substructures

MHD showed a generally moderate correlation with almost all dosimetric indices for each of the structures, reinforcing the broad applicability of the MHD metric (see Fig. 5). Correlation was stronger for larger structures (including the left and right ventricle, anterior and apical wall) that received higher radiation doses. MHD however was only poorly correlating to structures that received lower comparable doses (e.g. basal region), and for volumes that experienced a steep dose gradient (lateral ventricular wall, mid region). Correlation between MHD and selected individual segments (segments 7, 8, 13, 14, 15, 16 and 17) ranged from low to strong.

Discussion

This study presents the dosimetric values of several cardiac subvolumes in tangentially treated breast cancer patients, including the individual segments of the left ventricle using a novel contouring technique that seeks to report dose based on a well-known established cardiac standard [24]. This study confirms that doses within the left ventricle are heterogeneous, and are spatially and most accurately described by employing the AHA 17 segment model. It was found consistently that segments 7, 8, 13, 14, 15, 16 and 17 received the highest doses of radiation in both the free breathing breast/ chest wall only cohort, as well as those receiving nodal irradiation using DIBH, suggesting that there was minimal twisting or deformation of cardiac structures during breath hold. The reporting of radiation dosimetry in the AHA 17 segment model will allow direct pairing between radiation dose and pathologically affected segments of the left ventricle. One such imaging study has described left ventricular changes at the left ventricular regional level. Lo et al. [18] have confirmed apical left ventricular strain reductions following tangential breast irradiation and found a positive correlation to apical left ventricular dose. This same study has also reported statistically significant changes in individual left ventricular segment pre and post exposure to tangential radiation. The American Heart Association has also now recommended the reporting of abnormalities of the left ventricle with the 17 segment model [24] highlighting the need for a dosimetric equivalent. The novel contouring technique described in this study however was resource intensive (average contouring time per case was 60 min) and required specialised software, and hence translation into clinical practice for routine segmental dosimetric read out would be challenging in its current form. Incorporation however

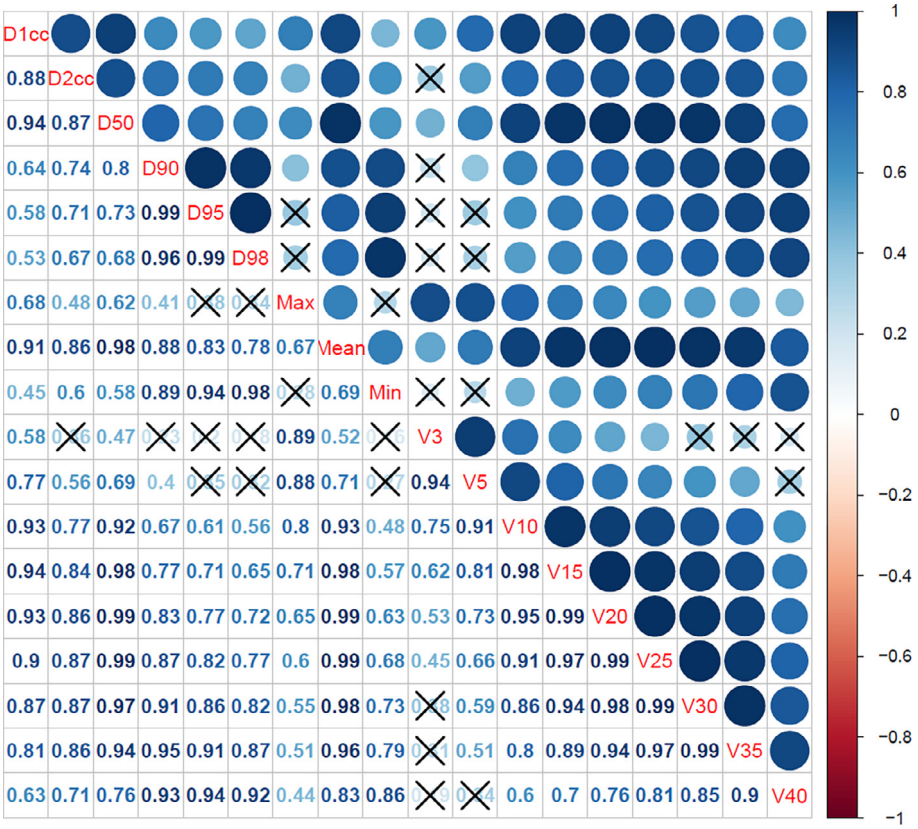

Fig. 4. Correlations between various dosimetric parameters of the whole heart. The correlation matrix demonstrates the mean heart dose (MHD) correlated highly or very highly with all dosimetric parameters except V3, minimum and maximum doses. Correlation of MHD almost reached parity with the D1cc, D50, V10, V15, V20, V25, V30, and V35 dosimetric parameters. D*x*cc – Dose delivered to *x* cubic centimetres. D*xx* – Dose delivered to *xx*% of the volume. Vxx – volume of defined region receiving *xx*Gy dose.

may be possible into a reference atlas for multi-atlas segmentation, which could improve contour efficiency, reduce inter-observer variability, and allow adoption into widespread clinical use [10].

Prior studies have either calculated cardiac doses using modelled patients with re-created 2D treatment fields [29], used set geometric rules [30] to define cardiac subvolumes, or used anatomical landmarks [31] to divide the heart in standard axial imaging planes. Therefore the primary strength of this study, in addition to the contouring of the left ventricular segment, was the rigour with which cardiac structures were delineated. Cardiac volumes were contoured in the cardiac planes, and independently reviewed by a cardiologist (JO). Segments of the left ventricle were contoured in the cardiac short axis, and divisions between cardiac regions and walls were verified in the 2 chamber and 4 chamber views. Therefore accurate contouring of the cardiac volumes was optimised. Interobserver variability was minimised due to a single observer (ST) contouring.

Limitations of the current study relate to the limited number of patients included, particularly those who underwent regional nodal irradiation and DIBH. Cardiac contouring was also performed on non ECG gated non contrast CT scan [31]. Organ motion during the cardiac and respiratory cycles only allowed radiation doses to the cardiac subvolumes (particularly to those of the individual segments) to be good approximations at best. Significant intraobserver and interobserver variability in cardiac contouring [14] has been described, although this issue was not specifically addressed, given that the focus of this study was to report absolute doses to cardiac subvolumes.

Erven et al. [17] have previously commented on segmenting the left ventricle into 18 segments although values to each segment were not reported. In our cohort of patients receiving breast only radiation, the anterior wall and apical regions received the highest doses with a median mean dose of 9.21 Gy and 14.99 Gy respectively, which differ from those published by Erven et al. Direct comparisons of doses however are difficult given Erven et al., included the ventricular blood pool in their volumetric analysis, segmented the left ventricle into 18 segments, and included the apical cap in their definition of the ventricular wall. Mean heart doses (2.62 Gy vs 9.00 Gy) and left ventricular doses (mean dose 4.53 Gy vs 9.00 Gy) were also lower in our study.

Correlation between the multiple dosimetric parameters of the whole heart showed a very high correlation between mean heart dose and all reported dosimetric parameters except V3, minimum and maximum doses. Correlation coefficients between MHD and several dosimetric parameters (D1cc, D50, V10, V15, V20, V25, V30, and V35) approached unity, and could be assumed as statistically equivalent. MHD correlated moderately well with doses to various subvolumes of the heart. Correlation coefficients ranged between 0.29 and 0.82, with lower correlation coefficients being seen in structures that were of small volume and experiencing a high degree of dose heterogeneity, exemplified best by the left anterior descending artery. Mean heart dose however was inadequately representative of left ventricular segments, with a predominantly weak to moderate correlation with the high dose left ventricular segments (particularly those of the anterior ventricular wall and apical region). This highlights the limitation of MHD in describing the dose profile in left ventricular segments and its utility when correlated with regional imaging defects.

Correlation of dosimetric indices within a subvolume demonstrated often strong correlations between mean dose and most

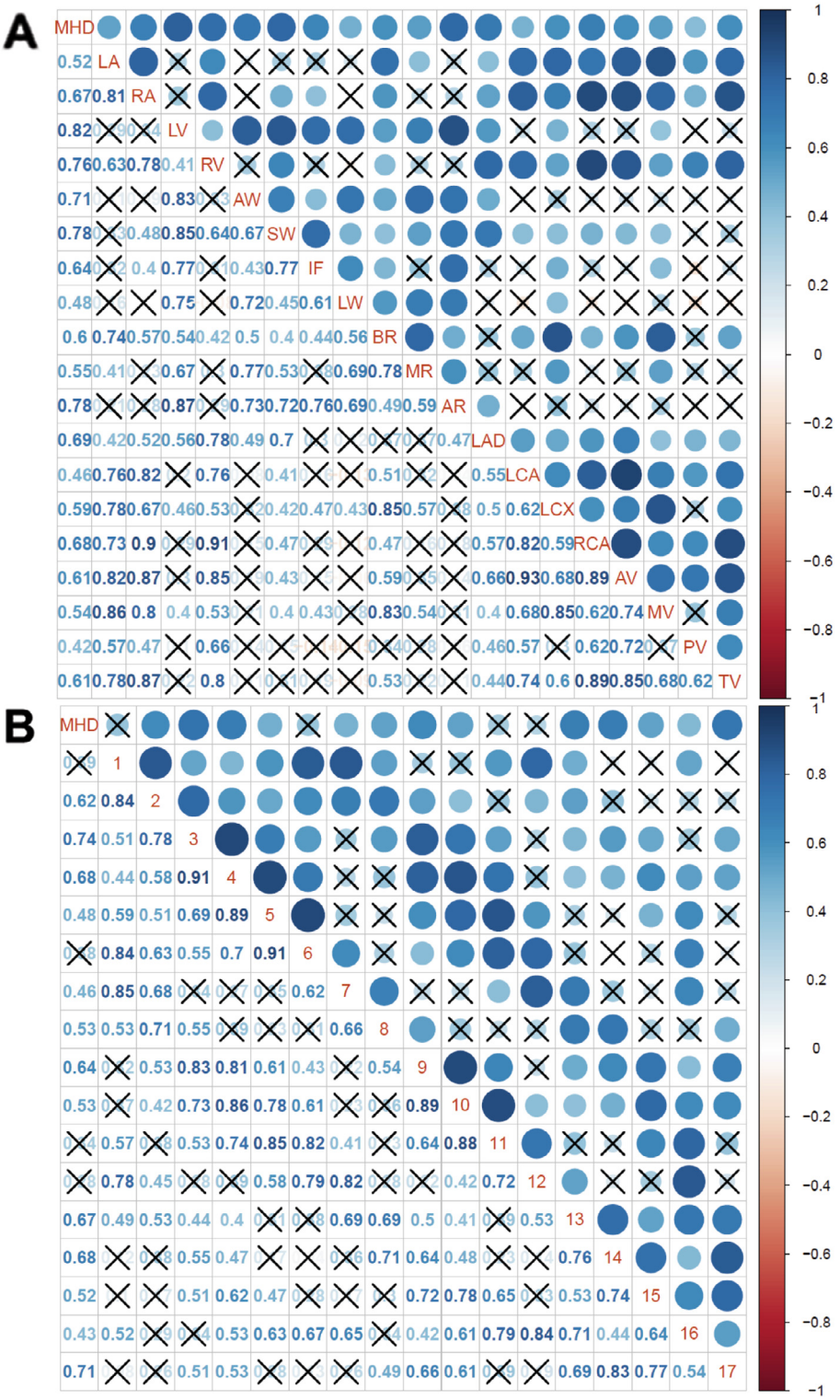

Fig. 5. Correlations between Mean Heart Dose and cardiac substructures (A) and ventricular segments (B) are depicted below. Fig. 5A shows correlation matrix between mean heart dose (MHD) and mean dose to various cardiac subvolumes. MHD correlated highly with the left and right ventricles, only moderately with the left and right atria. MHD correlated highly with the anterior and septal wall, and moderately with the inferior and lateral ventricular walls. MHD correlated highly with the apical region. MHD correlation with all coronary arteries was moderate. Correlation between MHD and cardiac valves was weak to moderate. Fig. 5B shows a correlation matrix between MHD and segments of the left ventricle. MHD correlated highly only with segment 17 (apical cap), with moderate correlations with the apical segments (anterior (13) septal (14)), mid inferoseptal (9) segment, and basal septal segments (anteroseptal (2), and inferoseptal (3)). All correlation values are significant $p \leq 0.05$. All crossed boxes are not statistically significant $p > 0.05$. MHD = Mean heart dose, LA = Left Atrium, RA = Right Atrium, LV = Left Ventricle, RV = Right Ventricle, AW = Anterior Wall, SW = Septal Wall, IF = Inferior Wall, LW = Lateral Wall, BR = Basal Region, MR = Mid Region, AR = Apical Region, LAD = Left Anterior Descending Artery, LCA = Left Coronary Artery, LCX – Left Circumflex Artery, RCA = Right Coronary Artery, AV = Aortic Valve, MV = Mitral Valve, PV = Pulmonary Valve, TV = Tricuspid Valve. Numbers 1 to 17 represent left ventricular segments.

dosimetric indices. Those that were more weakly correlated with the subvolume mean dose were often strongly correlated with maximum dose, and hence measurement of mean and maximum doses may provide a good foundation from which further exploratory dose analysis could be undertaken.

This study documents the use of a novel contouring technique to contour the cardiac substructures, and has demonstrated the feasibility of documenting radiation doses particularly to the left ventricle based on the AHA 17 segment model. Such reporting of specific regional dose delivery provides the most accurate spatial description of delivered radiation to the heart, particularly in breast cancer where the left ventricle is most frequently exposed. Mean heart dose was found to correlate moderately well with doses to most cardiac subvolumes, justifying its utility as the most commonly used cardiac dosimetric parameter. Correlation however of MHD was weak with segments of the left ventricle, limiting its utility to describe focal segmental left ventricular abnormalities with imaging. Future understanding of cardiotoxicity will require the precise matching of radiation dose to regional imaging defects [22], which are being reported evermore precisely, underscoring the need for detailed dose determination.

Disclosures

Simon Tang – recipient of the RANZCR research grant – awarded 20 000 AUD.

James Otton – No disclosures.

Lois Holloway – Liverpool Cancer Therapy Cancer has a research agreement with Siemens Medical Systems in relation to the MRI scanner used for the larger project associated with this manuscript.

Geoffrey Delaney – No disclosures.

Gary Liney – No disclosures.

Armia George – No disclosures.

Michael Jameson – No disclosures.

David Tran – No disclosures.

Vikneswary Batumalai – No disclosures.

Liza Thomas – No disclosures.

Eng-Siew Koh – No disclosures.

Conflict of interest statement

There are no conflicts of interest.

Appendix A. Supplementary data

Supplementary data to this article can be found online at https://doi.org/10.1016/j.radonc.2018.09.021.

References

[1] Cuzick J, Stewart H, Rutqvist L, Houghton J, Edwards R, Redmond C, et al. Cause-specific mortality in long-term survivors of breast cancer who participated in trials of radiotherapy. J Clin Oncol 1994;12:447–53.

[2] Taylor C, McGale P, Brønnum D, Correa C, Cutter D, Duane FK, et al. Cardiac structure injury after radiotherapy for breast cancer: cross-sectional study with individual patient data. J Clin Oncol 2018;36:2288–96.

[3] Harris EE, Correa C, Hwang WT, Liao J, Litt HI, Ferrari VA, et al. Late cardiac mortality and morbidity in early-stage breast cancer patients after breast-conservation treatment. J Clin Oncol 2006;24:4100–6.

[4] Darby SC, Ewertz M, McGale P, Bennet AM, Blom-Goldman U, Brønnum D, et al. Risk of ischemic heart disease in women after radiotherapy for breast cancer. N Engl J Med 2013;368:987–98.

[5] Boekel NB, Schaapveld M, Gietema JA, Russell NS, Poortmans P, Theuws JCM, et al. Cardiovascular disease risk in a large, population-based cohort of breast cancer survivors. Int J Radiat Oncol Biol Phys 2016(94):1061–72.

[6] Zhuang X-F, Yang Y-M, Sun X-L, Liao Z-K. Huang J: Late onset radiation-induced constrictive pericarditis and cardiomyopathy after radiotherapy: a case report. Medicine 2017;96:e5932.

[7] Gillette EL, McChesney SL, Hoopes PJ. Isoeffect curves for radiation-induced cardiomyopathy in the dog. Int J Radiat Oncol Biol Phys 1985;11:2091–7.

[8] Gagliardi G, Constine LS, Moiseenko V, Correa C, Pierce LJ, Allen AM, et al. Radiation dose–volume effects in the heart. Int J Radiat Oncol Biol Phys 2010;76(3, Supplement):S77–85.

[9] Taylor CW, Wang Z, Macaulay E, Jagsi R, Duane F, Darby SC. Exposure of the heart in breast cancer radiation therapy: a systematic review of heart doses published during 2003 to 2013. Int J Radiat Oncol Biol Phys 2015;93(4):845–53.

[10] Zhou R, Liao Z, Pan T, Milgrom SA, Pinnix CC, Shi A, et al. Cardiac atlas development and validation for automatic segmentation of cardiac substructures. Radiother Oncol 2017;122(1):66–71.

[11] Lo Q, Hee L, Batumalai V, Allman C, MacDonald P, Delaney GP, et al. Subclinical cardiac dysfunction detected by strain imaging during breast irradiation with persistent changes 6 weeks after treatment. Int J Radiat Oncol Biol Phys 2014;92:268–76.

[12] Darby SC, Cutter DJ, Boerma M, Constine LS, Fajardo LF, Kodama K, et al. Radiation-related heart disease: current knowledge and future prospects. Int J Radiat Oncol Biol Phys 2010;76(3):656–65.

[13] Bahig H, de Guise J, Vu T, Blais D, Chartrand-Lefebvre C, Nguyen NT, et al. In a heartbeat: an assessment of dynamic dose variation to cardiac structures using dual source computed tomography. Int J Radiat Oncol Biol Phys 2018.

[14] Feng M, Moran JM, Koelling T, Chughtai A, Chan JL, Freedman L, et al. Development and validation of a heart atlas to study cardiac exposure to radiation following treatment for breast cancer. Int J Radiat Oncol Biol Phys 2011;79:10–8.

[15] Hahn E, Jiang H, Ng A, Bashir S, Ahmed S, Tsang R, et al. Late cardiac toxicity after mediastinal radiation therapy for hodgkin lymphoma: contributions of coronary artery and whole heart dose-volume variables to risk prediction. Int J Radiat Oncol Biol Phys 2017;98:1116–23.

[16] van den Bogaard VA, Ta BD, van der Schaaf A, Bouma AB, Middag AM, Bantema-Joppe EJ, et al. Validation and modification of a prediction model for acute cardiac events in patients with breast cancer treated with radiotherapy based on three-dimensional dose distributions to cardiac substructures. J Clin Oncol 2017;35:1171–8.

[17] Erven K, Florian A, Slagmolen P, Sweldens C, Jurcut R, Wildiers H, et al. Subclinical cardiotoxicity detected by strain rate imaging up to 14 months after breast radiation therapy. Int J Radiat Oncol Biol Phys 2013;85:1172–8.

[18] Lo Q, Hee L, Batumalai V, Allman C, MacDonald P, Lonergan D, et al. Strain imaging detects dose-dependent segmental cardiac dysfunction in the acute phase after breast irradiation. Int J Radiat Oncol Biol Phys 2017;99:182–90.

[19] Marks LB, Yu X, Prosnitz RG, Zhou S-M, Hardenbergh PH, Blazing M, et al. The incidence and functional consequences of RT-associated cardiac perfusion defects. Int J Radiat Oncol Biol Phys 2005;63:214–23.

[20] Gyenes G, Fornander T, Carlens P, Glas U, Rutqvist LE. Myocardial damage in breast cancer patients treated with adjuvant radiotherapy: a prospective study. Int J Radiat Oncol Biol Phys 1996;36:899–905.

[21] Correa CR, Litt HI, Hwang W-T, Ferrari VA, Solin LJ, Harris EE. Coronary artery findings after left-sided compared with right-sided radiation treatment for early-stage breast cancer. J Clin Oncol: Official J Am Soc Clin Oncol 2007;25:3031–7.

[22] Duane F, Aznar MC, Bartlett F, Cutter DJ, Darby SC, Jagsi R, et al. A cardiac contouring atlas for radiotherapy. Radiother Oncol: J Eur Soc Therap Radiol Oncol 2017;122:416–22.

[23] McWilliam A, Kennedy J, Hodgson C, Vasquez Osorio E, Faivre-Finn C, van Herk M. Radiation dose to heart base linked with poorer survival in lung cancer patients. Eur J Cancer 2017;85:106–13.

[24] Cerqueira MD, Weissman NJ, Dilsizian V, Jacobs AK, Kaul S, Laskey WK, et al. Standardized myocardial segmentation and nomenclature for tomographic imaging of the heart. A Statement for Healthcare Professionals From the Cardiac Imaging Committee of the Council on Clinical Cardiology of the American Heart Association 2002;105:539–42.

[25] Lang RM, Badano LP, Mor-Avi V, Afilalo J, Armstrong A, Ernande L, et al. Recommendations for cardiac chamber quantification by echocardiography in adults: an update from the American Society of Echocardiography and the European Association of Cardiovascular Imaging. J Am Soc Echocardiography: Official Publ Am Soc Echocardiography 2015;28. 1-39.e14.

[26] Yang F, Minutello RM, Bhagan S, Sharma A, Wong SC. The impact of gender on vessel size in patients with angiographically normal coronary arteries. J Interventional Cardiol 2006;19:340–4.

[27] Erven K, Jurcut R, Weltens C, Giusca S, Ector J, Wildiers H, et al. Acute radiation effects on cardiac function detected by strain rate imaging in breast cancer patients. Int J Radiat Oncol Biol Phys 2011;79:1444–51.

[28] Mukaka MM. A guide to appropriate use of correlation coefficient in medical research. Malawi Med J: The J Med Assoc Malawi 2012;24:69–71.

[29] Taylor CW, Nisbet A, McGale P, Darby SC. Cardiac exposures in breast cancer radiotherapy: 1950s–1990s. Int J Radiat Oncol Biol Phys 2007;69:1484–95.

[30] Wollschlager D, Karle H, Stockinger M, Bartkowiak D, Buhrdel S, Merzenich H, et al. Radiation dose distribution in functional heart regions from tangential breast cancer radiotherapy. Radiother Oncol: J Eur Soc Therap Radiol Oncol 2016;119:65–70.

[31] Johansen S, Tjessem KH, Fossa K, Bosse G, Danielsen T, Malinen E, et al. Dose distribution in the heart and cardiac chambers following 4-field radiation therapy of breast cancer: a retrospective study. Breast Cancer: Basic Clin Res 2013;7:41–9.